

The Causes and Implications of Persistent Atmospheric CO₂ Biases in Earth System Models

Forrest M. Hoffman^{†‡}, James T. Randerson[†], and CMIP5 Carbon Cycle Model Leads

[†]Dept. of Earth System Sciences, University of California, Irvine; [‡]Computational Earth Sciences Group, Oak Ridge National Laboratory

Introduction

Increasing atmospheric carbon dioxide (CO₂) concentrations, resulting from anthropogenic perturbation of the global carbon cycle, are altering the Earth's climate. The strength of feedbacks between a changing climate and future CO₂ concentrations are highly uncertain and difficult to predict using Earth System Models (ESMs). To reduce the range of uncertainty in climate predictions, model representation of feedbacks must be improved through comparisons with contemporary observations. In this study, we analyzed emissions-driven simulations for historical (1850–2005) and future periods (Representative Concentration Pathway or RCP 8.5 for 2006–2100) produced by 13 ESMs for the Fifth Phase of the Coupled Model Intercomparison Project (CMIP5). We exploited a linear relationship found between the magnitude of contemporary and future atmospheric CO₂ levels to create a contemporary CO₂ tuned model (CCTM) estimate of the trajectory for the 21st century. This approach reduced the spread of future atmospheric CO₂ projections by a factor of 6.4 at 2060 and yielded radiative forcing and temperature increases during the 21st century that were lower than the multi-model mean.

Description of Models

Table 1: Models that generated output used in this study.

Model	Modeling Center (or Group)	Component Models and Resolutions	Atmosphere	Land	Ocean	Sea Ice
BCC-CSM1.1	Beijing Climate Center, China Meteorological Administration, CHINA	AGCM2.1 (T42L26)	AVIM1.0 (T42)	MOM4 L40 (tripolar, $1^\circ \times (1^\circ)^2$, L40)	SIS (tripolar, $1^\circ \times (1^\circ)^2$, L40)	
BCC-CSM1.1(m)	Beijing Climate Center, China Meteorological Administration, CHINA	AGCM2.1 (T42L26)	AVIM1.0 (T42)	MOM4 L40 (tripolar, $1^\circ \times (1^\circ)^2$, L40)	SIS (tripolar, $1^\circ \times (1^\circ)^2$, L40)	
BNU-ESM ^a	Beijing Normal University, CHINA	CA3.5 (T42L26)	CoLM + BNUDGVM (360 \times 200, L50)	MOM4p1 (360 \times 200)	OICE4.1 (360 \times 200)	
CanESM2 ^b (Arora et al., 2011)	Canadian Centre for Climate Modelling and Analysis, CANADA	CanAM4 (AGCM15, T63L35)	CLASS2.7 and CTEM1 (T42L10+5)	CanOM4 (OGCM4.0, 256 \times 192, L40) and CMOC1.2 (PQP2 gx1v6)	CansIM1 (T63)	
CESM1-BGC	Community Earth System Model Consortium, NSF-DOE-NCAR, USA	CAM4 (0.9° \times 1.25°)	CLM4 (0.9° \times 1.25°)	—	—	
FGOALS-s2 ^c	Institute of Atmospheric Physics, Chinese Academy of Sciences, CHINA	—	—	—	—	
GFDL-ESM2m ^d (Dunne et al., 2012, submitted)	NOAA Geophysical Fluid Dynamics Laboratory, USA	AM2 (2° \times 2.5°, L24)	LM3	MOM4 (tripolar, $1^\circ \times (1^\circ)^2$, L50)	SIS (tripolar, $1^\circ \times (1^\circ)^2$, L50)	
HadGEM2-ES ^e (Collins et al., 2011; Jones et al., 2011)	Met Office Hadley Centre, UNITED KINGDOM	HadGAM2 and UKCA (N96L38)	MOSES2 and TRIFFID	HadGCM2 and dia-HadGOC (1° \times 1°, L40)	—	
INM-CM4 ^f (Volodin et al., 2010)	Institute for Numerical Mathematics, RUSSIA	(2° \times 1.5°, L21)	—	(1° \times 0.5°, L40)	—	
IPSL-CM5A-LR ^g (Dufresne et al., submitted)	Institut Pierre-Simon Laplace, FRANCE	LMDZ4 (3.75° \times 1.9°, L39)	ORCHIDEE	ORCA2 and PISCES (2° \times 2.5°, L31)	LIM2	
MIROC-ESM ^h (Watanabe et al., 2011; Ouchies, 2001)	Japan Agency for Marine-Earth Science and Ocean Research, Atmosphere and Ocean Research Institute (The University of Tokyo), and National Institute of Environmental Studies, JAPAN	MIROC-AGCM (T42, L6)	MATIRO and SEIB-DGVM (T42L80)	COCCO3.4 and NPZD (256 \times 192, L44)	COCO3.4	
MPI-ESM1.0 ⁱ (Raddatz et al., 2007; Brovkin et al., 2009; Mahrer-Reimer et al., 2005)	Max Planck Institute for Meteorology, GERMANY	ECHAM6 (T63L47)	JSBACH	MIPO and HAMOCC (\sim 1.5°, L40)	4936	
MRI-ESM1	Meteorological Research Institute, JAPAN	GSMUV (T119L48)	HAL	MRI-COM3 (1° \times 0.5°, L51)	MRI-COM3	

^aAtmospheric CO₂ required unit correction.

^bOcean carbon flux required unit correction.

^cBNU-ESM provided no ocean cell area data.

^dFGOALS-s2 model provided no ocean carbon fluxes.

Observations and Calculations

- We used an observationally based estimate of anthropogenic CO₂ uptake by the ocean, produced by Khatiwala et al. (2009) using a Green's function model for ocean tracer transport, in combination with observed atmospheric CO₂ and fossil fuel emission estimates to assess model biases in carbon accumulation in the atmosphere, ocean, and land reservoirs.
- We adopted a strategy similar to that of Hall and Qu (2006) to constrain future trends in atmospheric CO₂ using contemporary observations to create the CCTM.
- We employed an impulse response function to estimate temperature changes based on time-integrated changes in radiative forcing to evaluate the implications of model CO₂ biases.

Contemporary Biases in Atmospheric CO₂

ESM Historical Atmospheric CO₂ Mole Fraction

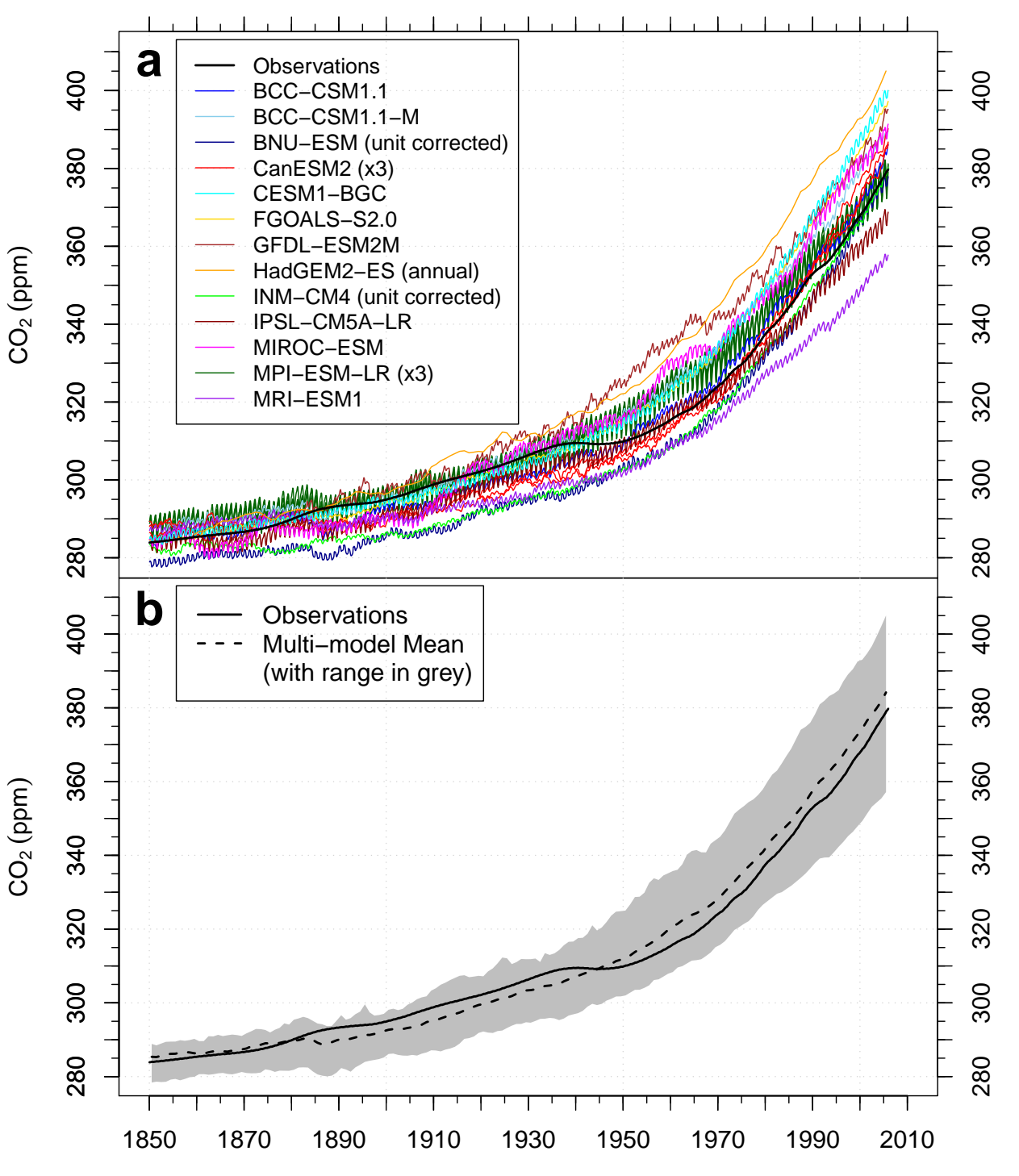


Figure 1(a): Most ESMs exhibit a high bias in atmospheric CO₂ mole fraction.

Figure 1(b): The multi-model mean is biased high from 1945 throughout the 20th century, ending 5.3 ppm above observations in 2005.

ESM Historical Ocean and Land Carbon Accumulation

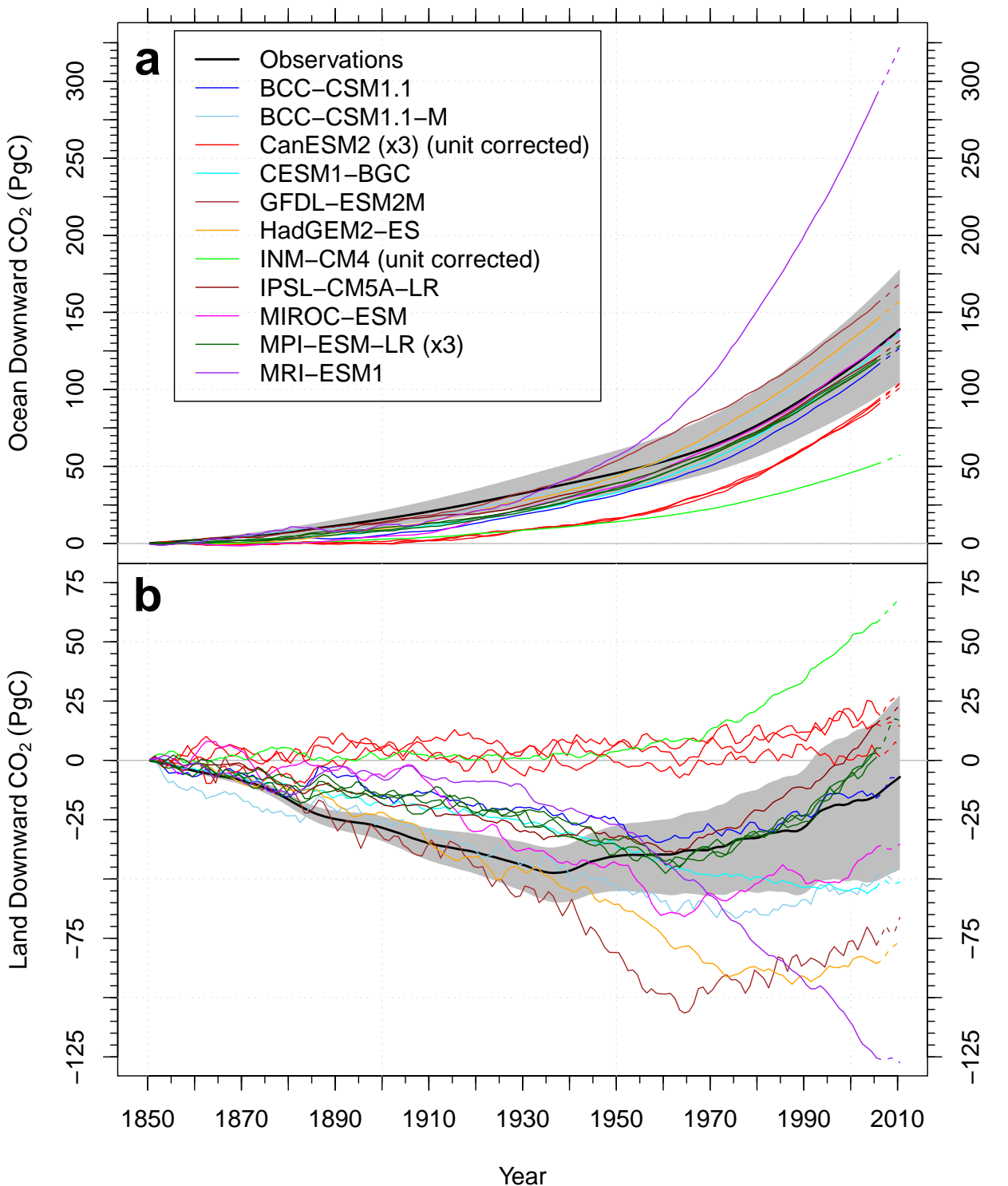


Figure 2(a): Ocean carbon accumulation from CMIP5 models ranged from 55–325 Pg C in 2010 as compared with adjusted estimates from Khatiwala et al. (2009).

Figure 2(b): CMIP5 models exhibit a wide range of land carbon accumulation responses, ranging from a cumulative net source of 125 Pg C to a sink of 75 Pg C in 2010.

Causes and Implications of the Contemporary Bias

- A key driver of the persistent high bias was weak ocean carbon uptake exhibited by the majority of ESMs.
- The high atmospheric CO₂ bias for the multi-model mean produced radiative forcing that was too large and, consequently, an unrealistically high temperature increase during the historical period.
- We will see that the atmospheric CO₂ bias persists into the future, causing large and divergent model projections during the 21st century.

Comparison with Khatiwala et al. (2009)

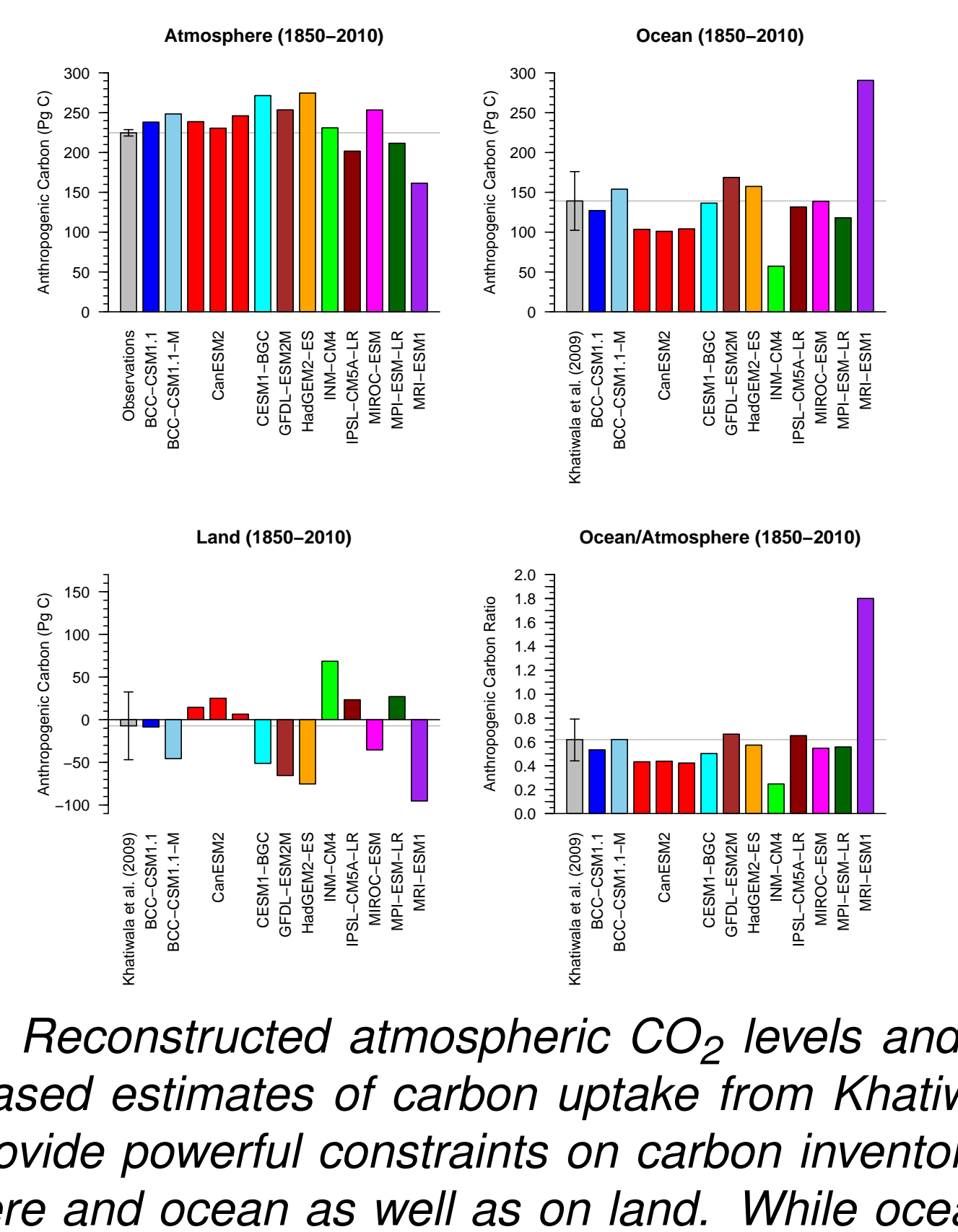


Figure 3: Reconstructed atmospheric CO₂ levels and observationally based estimates of carbon uptake from Khatiwala et al. (2009) provide powerful constraints on carbon inventories in the atmosphere and ocean as well as on land. While ocean carbon accumulation appears adequate in some model results, ocean carbon accumulation in most ESMs show a low bias once normalized by atmospheric accumulation (lower right panel).

Persistence of Biases into the Future

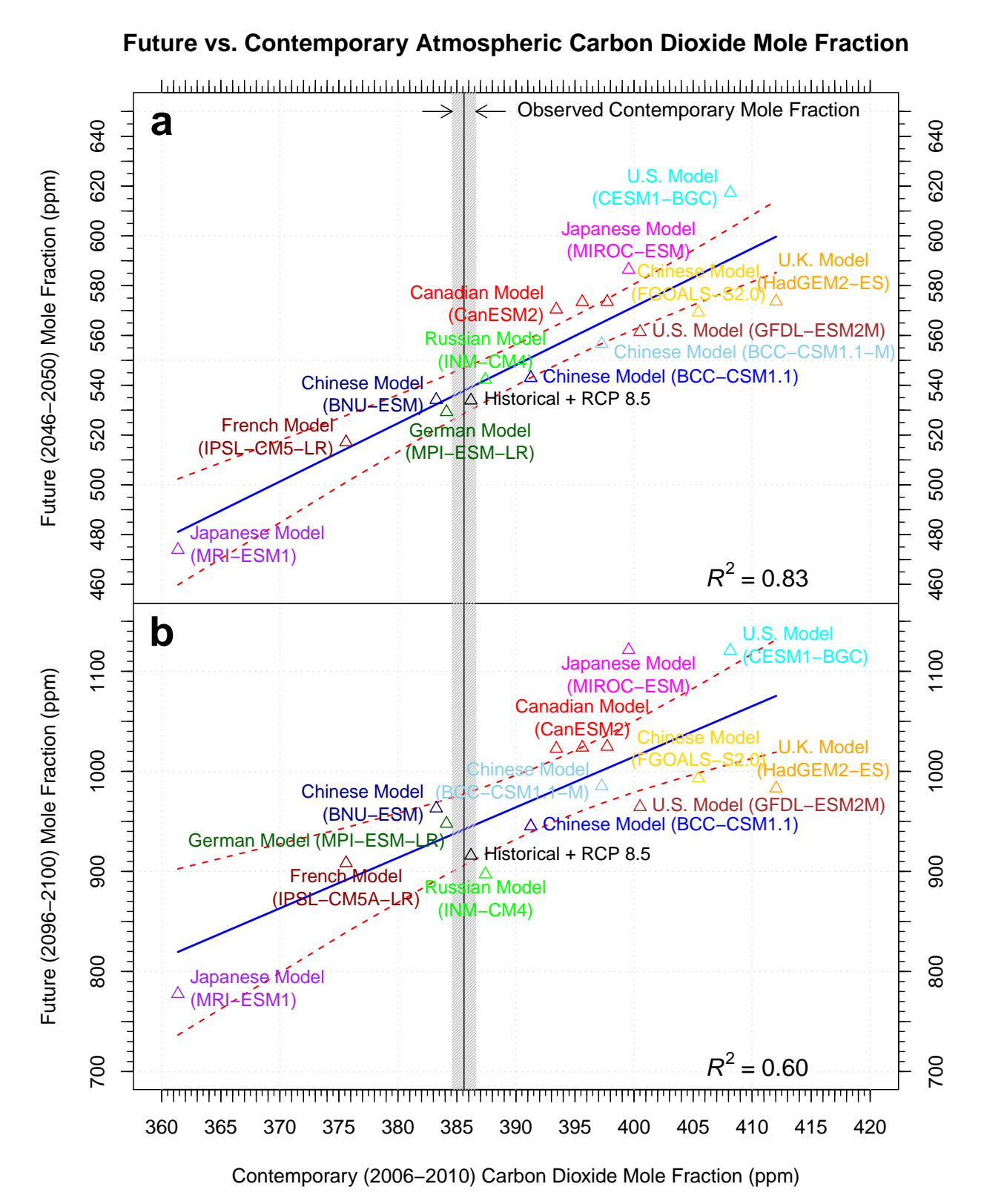


Figure 4: (a) Future (2050) vs. contemporary (2010) atmospheric CO₂ mole fraction fit for CMIP5 emissions-forced simulations of RCP 8.5. (b) Future (2100) vs. contemporary (2010) atmospheric CO₂ mole fraction fit for CMIP5 emissions-forced simulations of RCP 8.5.

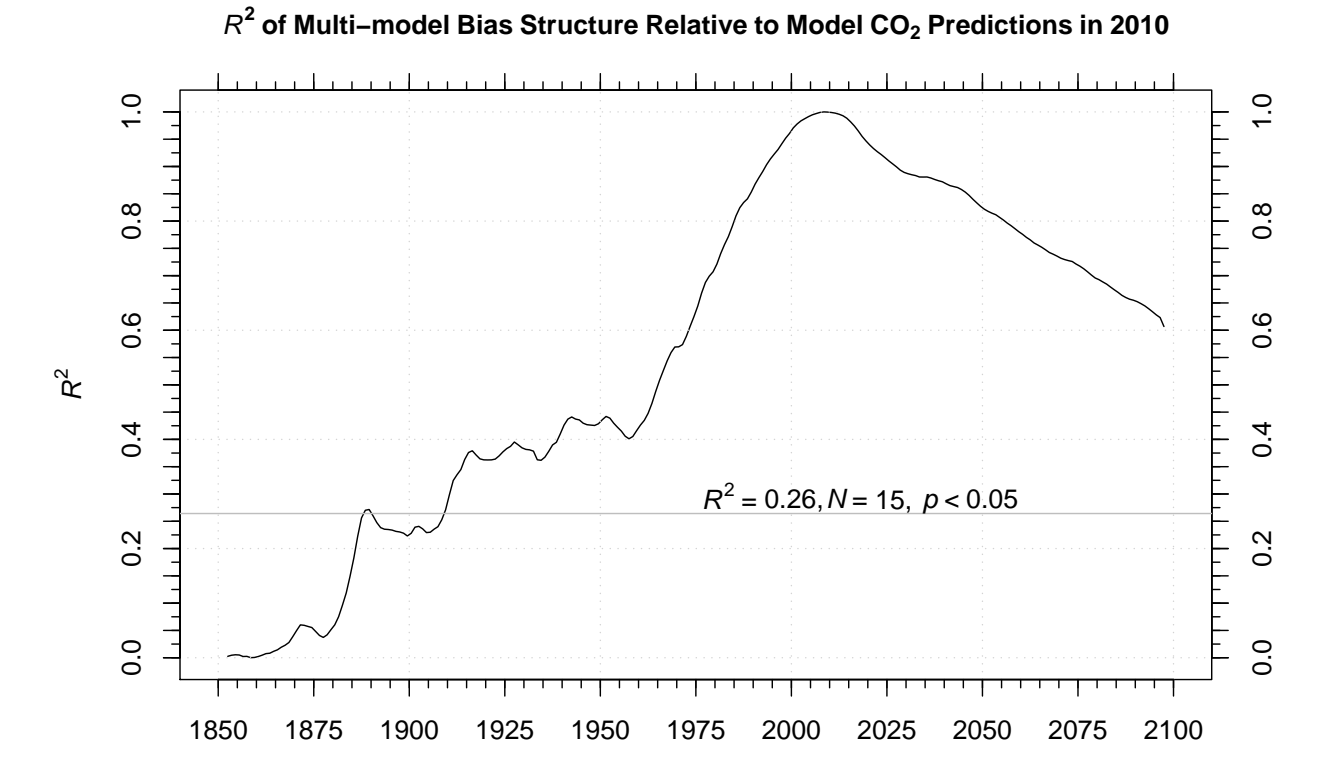


Figure 5: The coefficient of determination (R^2) for the multi-model bias structure relative to the set of CMIP5 model atmospheric CO₂ predictions at 2010.

Implications of a Persistent CO₂ Bias

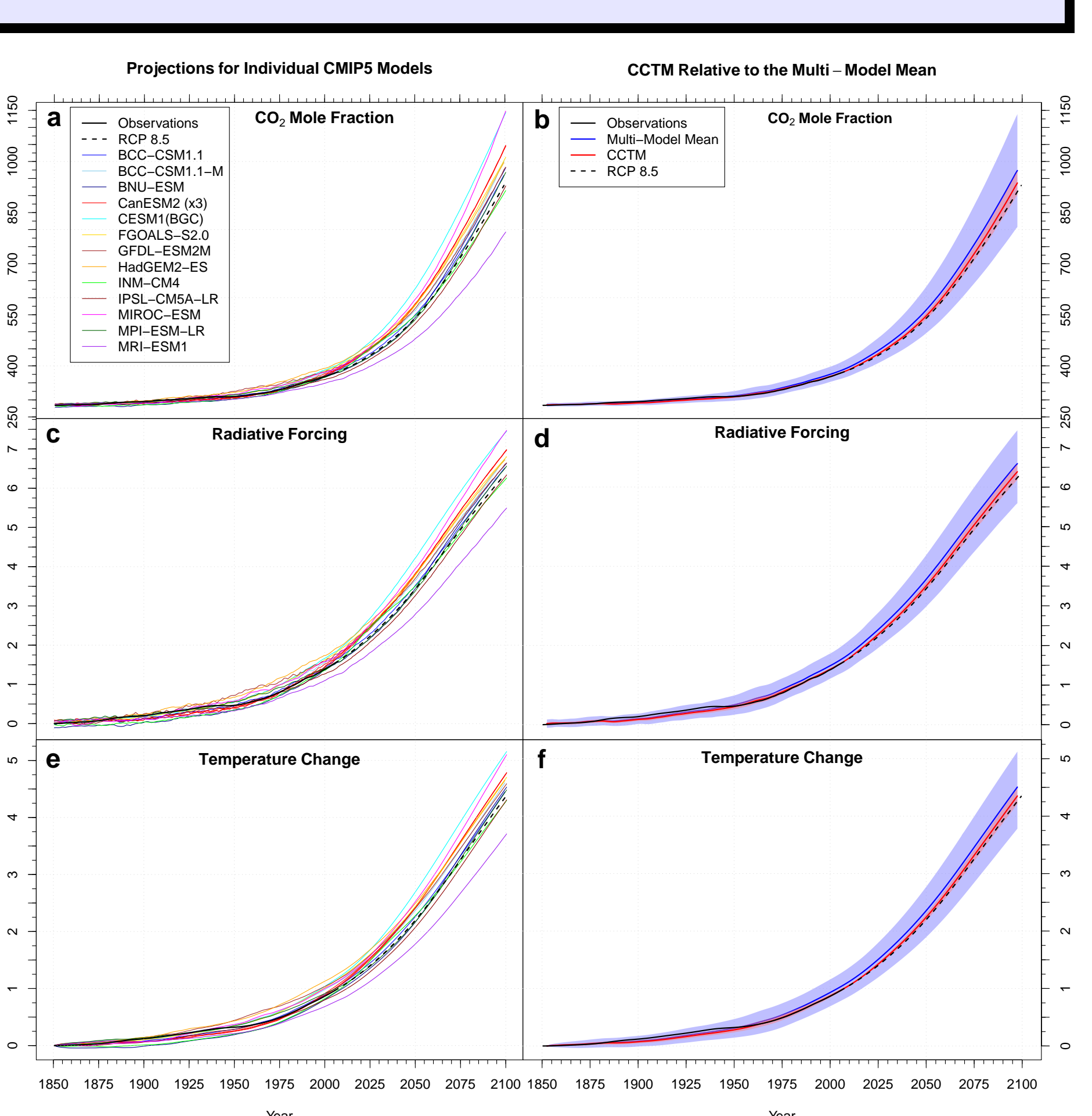


Figure 6: (a) CO₂ predictions for all CMIP5 models. (b) The contemporary CO₂ tuned model (CCTM) atmospheric CO₂ estimate compared to the CMIP5 multi-model mean trajectory. (c and d) Radiative forcing for all CMIP5 models and the CCTM. (e and f) Temperature changes for all CMIP5 models and the CCTM.

Table 2: Atmospheric CO₂ mole fraction, radiative forcing, and resulting temperature changes for each of the CMIP5 ESMs for the years 2010, 2060, and 2100. Values are 5-y means for the time periods 2006–2010, 2056–2060, and 2096–2100.

Model	CO ₂ Mole Fraction (ppm)		Radiative Forcing (W/m ⁻²)		Cumulative ΔT (°C)		ΔT (°C)
	2010	2060	2010	2060	2010	2060	
BCC-CSM1.1	390	603	945	1.70	4.03	6.43	1.06
BCC-CSM1.1-M	396	619	985	1.78	4.16	6.65	1.14
BNU-ESM	382	602	963	1.59	4.02	6.53	0.98
CanESM2 r1	394	641	1024	1.75	4.36	6.86	1.07
CanESM2 r2	392	641	1023	1.72	4.35	6.85	1.06
CanESM2 r3	396	641	1025	1.78	4.35	6.87	1.10
CESM1-BGC	407	697	1121	1.92	4.80	7.34	1.21
GFDL-ESM2	400	621	964	1.83	4.18	6.54	1.18
HadGEM2-ES	411	636	994	1.98	4.31	6.64	1.28
INM-CM4	386	591	897	1.64	3.92	6.15	1.00
IPSL-CM5A-LR	375	573	912	1.48	3.75	5.92	0.92
MIROC-ESM	398	651	1121	1.81	4.50	7.35	1.15
MIROC-ESM-LR	383	590	948	1.60	3.91	6.45	1.04
MRI-ESM1	361	516	778	1.28	3.20	5.39	0.81
Multi-model Mean	393	621	969	1.74	4.19	6.57	1.09
CCTM Estimate	386	601	932	1.64</			